NANO LETTERS

Letter

pubs.acs.org/NanoLett

The Influence of Substrate in Determining the Band Gap of Metallic Carbon Nanotubes

Moh. R. Amer,[†] Adam Bushmaker,[‡] and Stephen B. Cronin*,[†]

[†]Department of Electrical Engineering, University of Southern California, Los Angeles, California 90089, United States

[‡]The Aerospace Corporation, El Segundo, California 90245, United States

ABSTRACT: We report a detailed comparison of ultraclean suspended and on-substrate carbon nanotubes (CNTs) in order to quantify the effect of the substrate interaction on the effective band gap of metallic nanotubes. Here, individual CNTs are grown across two sets of electrodes, resulting in one segment of the nanotube that is suspended across a trench and the other segment supported on the substrate. The suspended segment shows a significant change in the conductance ($\Delta G/G = 0.84$) with applied gate voltage, which is attributed to a small band gap. The on-substrate segment, however, only shows a change in the measured conductance of $\Delta G/G = 0.11$. A Landauer model is used to fit the low bias conductance of these devices. From these fits, the band gaps in the suspended region range from 75 to 100 meV but are only 5−14.3 meV when the nanotube is in contact with the substrate. The decreased band gap is attributed to localized doping caused by trapped charges in the substrate that result in inhomogeneous broadening of the Fermi energy, which in turn limits the ability to modulate the conductance.

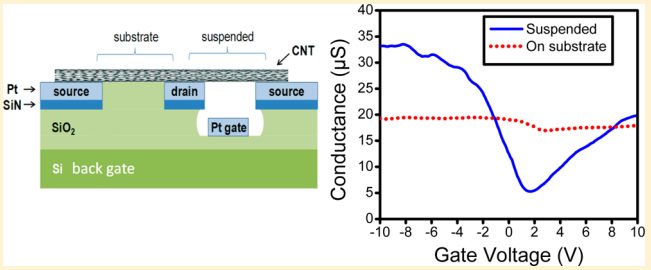

KEYWORDS: *Conductance, band gap, quasi-metallic, energy dispersion relation*

Metallic carbon nanotubes are known to exhibit small band gaps on the order of 10−100 meV.[1] The origin and magnitude of these band gaps, however, is still a topic of debate. Early scanning tunneling microscopy (STM) studies of metallic nanotubes attributed these small energy gaps to the curvature of the nanotube.[2] Tight binding calculations for armchair and metallic zigzag nanotubes do not predict the existence of a band gap in the electronic structure.[3] More recent calculations of metallic nanotubes show a small band gap caused by breaking of the bond symmetry due to curvature.[2,4−6] Uniaxial strain can also result in a band gap in metallic nanotube.[7,8] These types of symmetry-breaking band gaps (i.e., strain-induced, curvature-induced), however, can be closed with the application of an axial magnetic field. This, however, was not observed experimentally,[1] indicating that another underlying mechanism is responsible for the observed band gaps. The relatively large band gaps observed in ultraclean, suspended small gap metallic (i.e., quasi-metallic) carbon nanotubes have been attributed to a Mott insulator transition arising from strong electron−electron interactions.[1] However, this mechanism has not been confirmed by other experiments, and the exact nature of the Mott state is not known, whether it exhibits a charge density wave, spin density wave, or otherwise.[9,10] A large suppression of the Raman intensity has been correlated to the magnitude of the band gap in quasi-metallic nanotubes, which could result from a lattice distortion induced by a charge density wave.[11] Another possible mechanism for the observed energy gap is a Peierls distortion,[12] which results from strong electron−phonon interactions. First principles calculations have predicted a Peierls transition at temperatures as high as 300 K[13] for small diameter metallic CNTs with band gaps in the order of 0.25 eV.[14] While a Peierls distortion would result in a band gap and a large modulation of the Raman intensity through a lowering of the crystal symmetry, it has been predicted theoretically only in nanotubes with very small diameters and is not expected to occur in the relatively large diameter nanotubes grown in most experimental studies. Several phenomena have been observed in these ultraclean, suspended, nearly defect-free, metallic carbon nanotubes near zero gate voltage, including breakdown of the Born−Oppenheimer approximation (BOA),[15] thermal nonequilibrium phonon populations,[16] and large Raman intensity modulations.[11] Yet, to date, no detailed comparison of these band gaps on- and off-substrate has been made.

In this work, we perform a detailed comparison of CNTs grown on- and off-substrate in order to quantify the effect of the substrate interaction on the band gap of quasi-metallic nanotubes. We grow CNTs across two sets of electrodes, resulting in one segment of the nanotube suspended across a trench and the other segment supported on the substrate, as shown in Figure 1a,b. By comparing the band gaps of the same exact nanotube on- and off-substrate, we eliminate the variations associated with different nanotube chiralities and growth conditions. We then characterize the band gaps of these samples by fitting the $I-V_{gate}$ characteristics to a Landauer

   dx.doi.org/10.1021/nl302321k | *Nano Lett.* XXXX, XXX, XXX−XXX

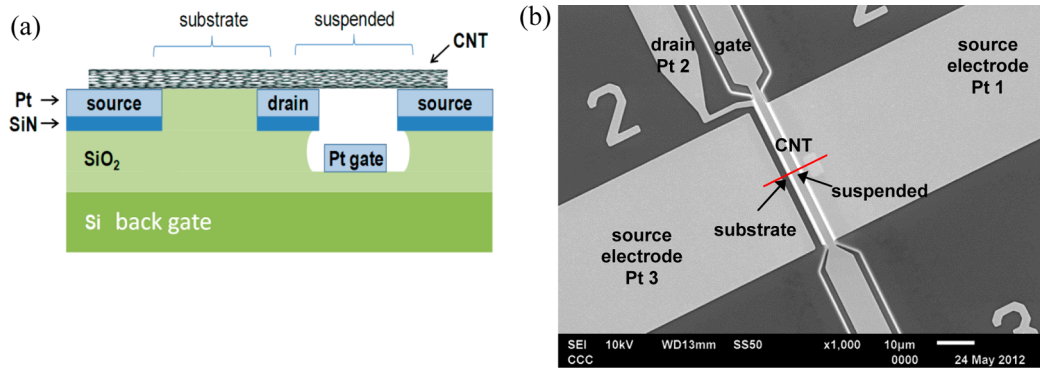

Figure 1. (a) Cross-sectional diagram and (b) SEM image of a carbon nanotube sample for comparing on-substrate and suspended CNT devices.

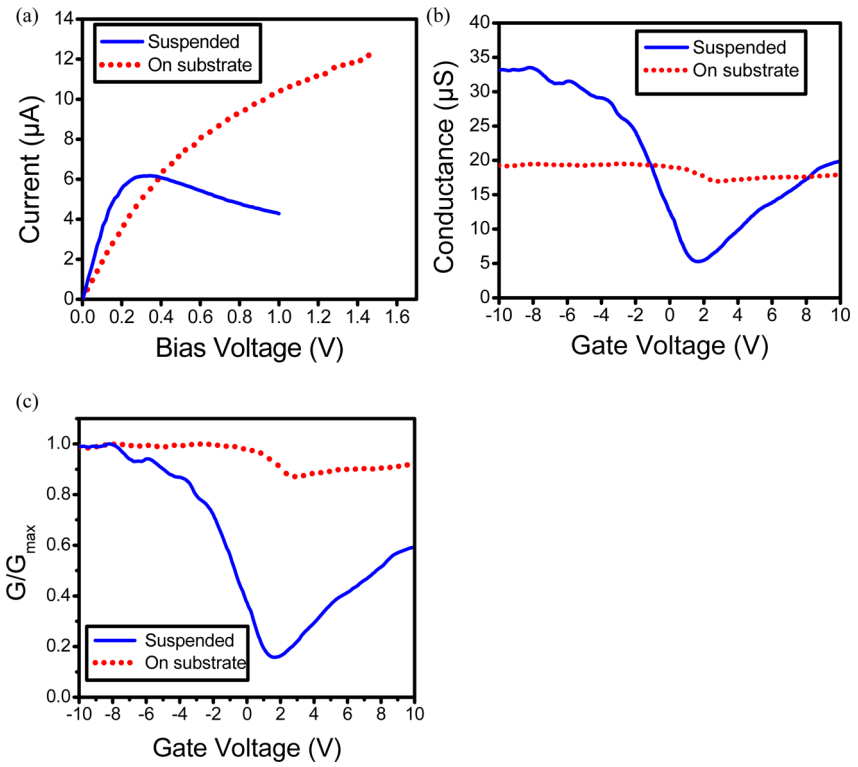

Figure 2. (a) $I-V_{bias}$ characteristics of the suspended and on-substrate regions taken from the same nanotube. The blue solid curve is for the suspended portion and the red dashed curve is for the on substrate portion. (b) $I-V_{gate}$ characteristics of the suspended and on-substrate regions. (c) Normalized conductance (G/G_{max}) plotted as a function of gate voltage.

transport model in order to identify the effect of the substrate on the electronic properties of quasi-metallic nanotubes.

Devices in this study are fabricated by first etching a 500 nm deep trench in a $Si/SiO_2/SiN$ substrate. Pt electrodes are patterned on top of the substrate using photolithography. Iron nanoparticle catalyst is then deposited on top of one of the electrodes close to the trench, as shown schematically in Figure 1a. Carbon nanotube growth is carried out at 875 °C for 15 min by flowing a mixture of argon, ethanol, and hydrogen. Figure 1b shows a scanning electron microscope (SEM) image of a final device. The $I-V_{bias}$ characteristics of the suspended CNT device are used to ensure that the device consists of only one nanotube, if the maximum current (in μA) satisfies the approximate relation $I_{max} \sim 10/L$, where L is the length of the nanotube, as established by Pop et al.[17]

Figure 2a shows the measured $I-V_{bias}$ of a metallic nanotube on and off the substrate. Negative differential conductance (NDC) appears for the suspended segment due to substantial heating of the nanotube by optical phonon emission.[16,17] The monotonic increase in current observed for the on-substrate segment indicates heat dissipation to the underlying substrate.[18] Figure 2b shows the measured conductance of the suspended and on-substrate segments plotted as a function of gate voltage. We used the Pt gate electrode to measure the conductance of the suspended segment while the Si back gate was used to measure the on substrate segment. For the suspended segment of the nanotube, the measured conductance drops from 33.1 μS at $V_g = -10$ V to 5.3 μS at the charge neutrality point, giving a conductance modulation of $\Delta G/G = 0.84$. Whereas, for the on-substrate segment, the conductance changes by only $\Delta G/G = 0.11$. In order to illustrate the drastic difference in conductance of each nanotube segment, Figure 2c shows the normalized conductance of each segment as a function of gate voltage. This difference in conductance is attributed to an effective reduction

dx.doi.org/10.1021/nl302321k | Nano Lett. XXXX, XXX, XXX–XXX

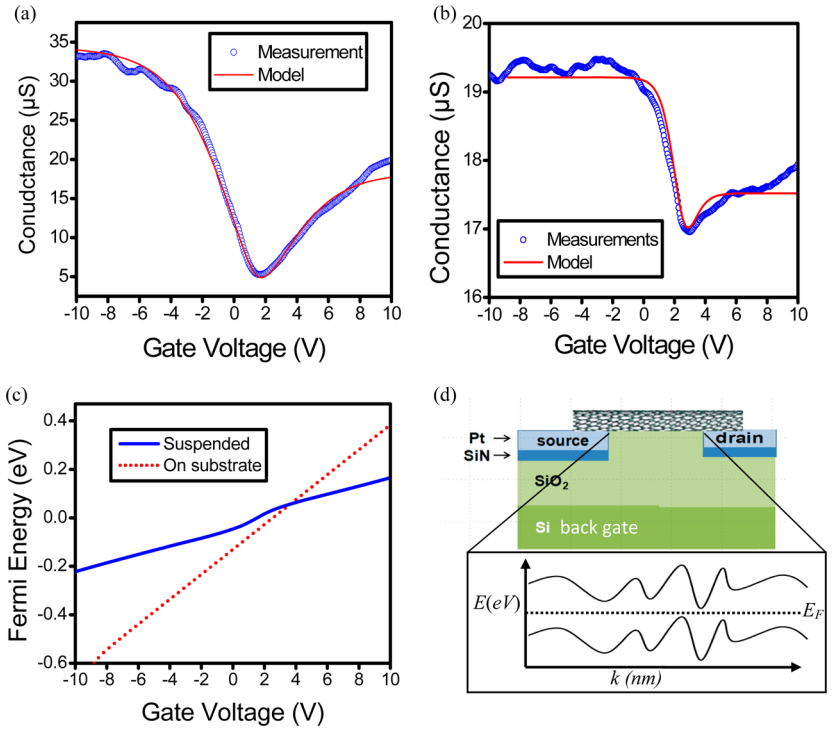

Figure 3. The measured conductance (open blue circles) fitted to the Landauer model (red curve) for (a) suspended and (b) on-substrate segments of the nanotube. (c) The relation between the Fermi energy and gate voltage for the suspended and on-substrate segments. (d) Schematic diagram illustrating the spatial fluctuations of the energy bands due to the trapped charges in the nanotube obscuring the mini-gap.

of the band gap in the metallic nanotube when it is in contact with the substrate. We believe the primary effect of the substrate in determining the effective band gap is trapped charges. Other effects, such as diameter deformation, can also lead to change in the band gap.[19] However, these changes would result in a decrease in band gap for some chiralities and an increase for others, which is not observed experimentally. In order to quantify the changes observed in the effective band gap, we fit the $I-V_{gate}$ data using a Landuaer model, as discussed previously.[16] Briefly, the low bias conductance of the device can be expressed as

$$G = \left(\frac{4e^2}{h}\right)\int_{-\infty}^{\infty}\left(\frac{\lambda_{eff}}{\lambda_{eff}+L}\right)\left(\frac{-\partial f}{\partial E}\right)dE \quad (1)$$

where λ_{eff} is the effective mean free path (given by Matthiessen rule), L is the device length, and $\partial f/\partial E$ is the derivative of the Fermi–Dirac distribution.[20] Using a hyperbolic energy dispersion relation, we integrate over the density of states which is given by

$$D(E) = \sum_{J=1}^{N}\left|\frac{dE_J(k)}{dk}\right|^{-1} \quad (2)$$

Here, the density of states is zero inside the band gap, E_g. Figure 3a shows a fit of the suspended $I-V_{gate}$ characteristics using this model with E_g = 100 meV. Using the same nanotube parameters in the fit (i.e., diameter), the on-substrate data is fitted by decreasing the band gap of the device to E_g = 5 meV, as shown in Figure 3b.

The Fermi energy in the nanotube is related to the applied gate voltage according to the following relation:[16,21,22]

$$E_F + \frac{Q}{C} = eV_{gate} \quad (3)$$

where E_F is the Fermi energy, Q is the electric charge on the nanotube, and C is the geometric capacitance. In our initial fits, the capacitance per unit length was calculated using the formula $C' = 2\pi\varepsilon_r\varepsilon_o/\ln(4h/d_t)$, where h and d_t are the dielectric thickness (1 μm) and the nanotube diameter (1.3 nm), respectively.[23] From the schematic diagram of Figure 1a, the gates for the on-substrate and suspended segments are structurally different. This geometric difference can significantly affect the capacitive coupling and gating effect. These different geometries result in capacitance values of 8.05 and 20.6 pF/μm for the suspended and on-substrate segments, respectively. We found that these fits could be improved by decreasing these capacitance values to 7 and 10 pF/μm. While these changes in the capacitance improve the fits, they do not change the value of the band gap, which is strongly affected by the relative value of minimum conductance $\Delta G/G$. Figure 3c shows the Fermi energy plotted as a function of the gate voltage, using the band gap and capacitance values in eqs 2 and 3. The Fermi energy of the suspended segment exhibits significant nonlinear behavior due to its relatively large band gap (E_g = 100 meV), while the on-substrate Fermi energy shows almost linear behavior, as expected for a metallic nanotube with little or no band gap. In Table 1, we list the change in conductance and band gaps of four samples measured using this approach.

We believe this reduction in the effective band gap is due to localized doping of the nanotube by trapped charges in the substrate, which results in a spatially varying Fermi energy, as illustrated schematically in Figure 3d. This results in an inhomogeneous broadening of the Fermi energy, as illustrated schematically in Figure 3d. The spatial variation of the Fermi energy in graphene on SiO_2 and hexagonal boron nitride has

dx.doi.org/10.1021/nl302321k | Nano Lett. XXXX, XXX, XXX–XXX

Table 1. The Extracted Band Gap and Conductivity Modulation of the Suspended and on Substrate Regions for Four Different Samples

sample	suspended band gap (meV)	$(\Delta G/G_{max})_{suspended}$	on substrate band gap (meV)	$(\Delta G/G_{max})_{substrate}$
sample 1	100	0.84	5	0.111
sample 2	90	0.76	14.3	0.28
sample 3	75	0.75	9.6	0.134
sample 4	90	0.82	5.1	0.158

recently been mapped using scanning tunneling microscopy (STM).[24] On SiO_2, the local Fermi energy was found to vary by as much as 100 meV, which is consistent with our measurements on carbon nanotube devices. It is these fluctuations in the Fermi energy that have made it difficult to observe the band gap in bilayer graphene, unless it is deposited on *h*-BN.[25] The effective band gaps extracted from the Landauer model are the result of the substrate obscuring the band gap rather than an inherent modulation of the intrinsic band gap of the nanotube. The appropriate interpretation is that all metallic carbon nanotubes have large band gaps that are typically obscured by the fluctuations in the local Fermi energy when supported by a Si/SiO_2 substrate.

The large effective band gaps observed in the conductance of the suspended segment is the breaking of the crystal symmetry due to curvature. Theoretically, the curvature induced band gap of a 1.3 nm diameter nanotube has been predicted to lie between 26 and 35 meV,[4,26] which is 3−4 times smaller than the band gaps reported in Table 1 for the suspended segment. This particular region may exhibit curvature induced band gap as a secondary effect but there may be other phenomenon contributing to the large band gaps, as described in the introduction of this paper.

In conclusion, we have characterized carbon nanotube devices with one segment of the nanotube suspended and the other segment lying on the substrate. The suspended segment shows a significant change in the conductance ($\Delta G/G = 0.84$) as a function of gate voltage, while the on-substrate segment shows a small change of $\Delta G/G = 0.11$. A Landauer model is used to fit the effective band gap of each segment, resulting in values that range between 75 and 100 meV for the suspended segment and 5−14.3 meV for the on-substrate segment. This change in the effective band gap is attributed to an alteration in the electronic properties of the nanotube due to trapped charges in the substrate, which creates fluctuations in the Fermi energy.

AUTHOR INFORMATION

Corresponding Author
*E-mail: scronin@usc.edu.

ACKNOWLEDGMENTS

This work was supported in part by Department of Energy (DOE) Award No. DE-FG02-07ER46376 and Office of Naval Research (ONR) Award No. N000141010511. A portion of this work was carried out in the University of California Santa Barbara (UCSB) nanofabrication facility, part of the NSF funded National Nanotechnology Infrastructure Network (NNIN) network. The portion of the work done at The Aerospace Corporation was funded by the Independent Research and Development program at The Aerospace Corporation.

REFERENCES

(1) Deshpande, V. V.; Chandra, B.; Caldwell, R.; Novikov, D. S.; Hone, J.; Bockrath, M. Mott insulating state in ultraclean carbon nanotubes. *Science* **2009**, *323*, 106−110.
(2) Ouyang, M.; Huang, J. L.; Cheung, C. L.; Lieber, C. M. Energy gaps in "metallic" single-walled carbon nanotubes. *Science* **2001**, *292*, 702−705.
(3) Saito, R.; Dresselhaus, G.; Dresselhaus, M. S. *Physical properties of carbon nanotubes*; World Scientific: New York, 1998; Vol. *35*.
(4) Charlier, J. C.; Blase, X.; Roche, S. Electronic and transport properties of nanotubes. *Rev. Mod. Phys.* **2007**, *79*, 677.
(5) Kane, C. L.; Mele, E. Size, shape, and low energy electronic structure of carbon nanotubes. *Phys. Rev. Lett.* **1997**, *78*, 1932−1935.
(6) Kleiner, A.; Eggert, S. Band gaps of primary metallic carbon nanotubes. *Phys. Rev. B* **2001**, *63*, 073408.
(7) Yang, L.; Anantram, M.; Han, J.; Lu, J. Band-gap change of carbon nanotubes: Effect of small uniaxial and torsional strain. *Phys. Rev. B* **1999**, *60*, 13874.
(8) Cronin, S.; Swan, A.; Ünlü, M.; Goldberg, B.; Dresselhaus, M.; Tinkham, M. Resonant Raman spectroscopy of individual metallic and semiconducting single-wall carbon nanotubes under uniaxial strain. *Phys. Rev. B* **2005**, *72*, 035425.
(9) Krotov, Y. A.; Lee, D. H.; Louie, S. G. Low energy properties of (n, n) carbon nanotubes. *Phys. Rev. Lett.* **1997**, *78*, 4245−4248.
(10) Balents, L.; Fisher, M. P. A. Correlation effects in carbon nanotubes. *Phys. Rev. B* **1997**, *55*, 11973−11976.
(11) Bushmaker, A. W.; Deshpande, V. V.; Hsieh, S.; Bockrath, M. W.; Cronin, S. B. Large Modulations in the Intensity of Raman-Scattered Light from Pristine Carbon Nanotubes. *Phys. Rev. Lett.* **2009**, *103*, 67401.
(12) Piscanec, S.; Lazzeri, M.; Robertson, J.; Ferrari, A. C.; Mauri, F. Optical phonons in carbon nanotubes: Kohn anomalies, Peierls distortions, and dynamic effects. *Phys. Rev. B* **2007**, *75*, 035427.
(13) Connétable, D.; Rignanese, G. M.; Charlier, J. C.; Blase, X. Room temperature Peierls distortion in small diameter nanotubes. *Phys. Rev. Lett.* **2005**, *94*, 15503.
(14) Dumont, G.; Boulanger, P.; Côté, M.; Ernzerhof, M. Peierls instability in carbon nanotubes: A first-principles study. *Phys. Rev. B* **2010**, *82*, 035419.
(15) Bushmaker, A. W.; Deshpande, V. V.; Hsieh, S.; Bockrath, M. W.; Cronin, S. B. Direct Observation of Born Oppenheimer Approximation Breakdown in Carbon Nanotubes. *Nano Lett.* **2009**, *9*, 607−611.
(16) Bushmaker, A. W.; Deshpande, V. V.; Hsieh, S.; Bockrath, M. W.; Cronin, S. B. Gate Voltage Controllable Non-Equilibrium and Non-Ohmic Behavior in Suspended Carbon Nanotubes. *Nano Lett.* **2009**, *9*, 2862−2866.
(17) Pop, E.; Mann, D.; Cao, J.; Wang, Q.; Goodson, K.; Dai, H. Negative differential conductance and hot phonons in suspended nanotube molecular wires. *Phys. Rev. Lett.* **2005**, *95*, 155505.
(18) Yao, Z.; Kane, C.; Dekker, C. High-field electrical transport in single-wall carbon nanotubes. *Phys. Rev. Lett.* **2000**, *84*, 2941−2944.
(19) Park, C. J.; Kim, Y. H.; Chang, K. Band-gap modification by radial deformation in carbon nanotubes. *Phys. Rev. B* **1999**, *60*, 10656.
(20) Zhao, Y.; Liao, A.; Pop, E. Multiband mobility in semiconducting carbon nanotubes. *IEEE Electron Device Lett.* **2009**, *30*, 1078−1080.
(21) Das, A.; Pisana, S.; Chakraborty, B.; Piscanec, S.; Saha, S.; Waghmare, U.; Novoselov, K.; Krishnamurthy, H.; Geim, A.; Ferrari, A. Monitoring dopants by Raman scattering in an electrochemically top-gated graphene transistor. *Nat. Nanotechnol.* **2008**, *3*, 210−215.
(22) Bushmaker, A.; Chang, C.; Deshpande, V.; Amer, M.; Bockrath, M.; Cronin, S. Memristive Behavior Observed in Defected Single-Walled Carbon Nanotubes. *IEEE Trans. Nanotechnol.* **2011**, 1−1.
(23) Rosenblatt, S.; Yaish, Y.; Park, J.; Gore, J.; Sazonova, V.; McEuen, P. L. High-Performance Electrolyte Gated Carbon Nanotube Transistors. *Nano Lett.* **2002**, *2*, 869−872.
(24) Xue, J.; Sanchez-Yamagishi, J.; Bulmash, D.; Jacquod, P.; Deshpande, A.; Watanabe, K.; Taniguchi, T.; Jarillo-Herrero, P.;

LeRoy, B. J. Scanning tunnelling microscopy and spectroscopy of ultra-flat graphene on hexagonal boron nitride. *Nat. mater.* **2011**, *10*, 282−285.
(25) Dean, C.; Young, A.; Meric, I.; Lee, C.; Wang, L.; Sorgenfrei, S.; Watanabe, K.; Taniguchi, T.; Kim, P.; Shepard, K. Boron nitride substrates for high-quality graphene electronics. *Nat. nanotechnol.* **2010**, *5*, 722−726.
(26) Sasaki, K.; Saito, R.; Dresselhaus, G.; Dresselhaus, M. S.; Farhat, H.; Kong, J. Curvature-induced optical phonon frequency shift in metallic carbon nanotubes. *Phys. Rev. B* **2008**, *77*, 245441.

dx.doi.org/10.1021/nl302321k | *Nano Lett.* XXXX, XXX, XXX−XXX